In Rat Dorsal Root Ganglion Neurons, Herpes Simplex Virus Type 1 Tegument Forms in the Cytoplasm of the Cell Body

Monica Miranda-Saksena,[1] Ross A. Boadle,[2] Patricia Armati,[3] and Anthony L. Cunningham[1]*

Centre for Virus Research[1] and Electron Microscope Laboratory, Institute of Clinical Pathology and Medical Research,[2] Westmead Millennium Institute, Westmead Hospital and University of Sydney, Westmead, New South Wales 2145, and School of Biological Sciences, University of Sydney, Camperdown, New South Wales 2050,[3] Australia

The herpes simplex virus type 1 (HSV-1) tegument is the least understood component of the virion, and the mechanism of tegument assembly and incorporation into virions during viral egress has not yet been elucidated. In the present study, the addition of tegument proteins (VP13/14, VP16, VP22, and US9) and envelope glycoproteins (gD and gH) to herpes simplex virions in the cell body of rat dorsal root ganglion neurons was examined by immunoelectron microscopy. All tegument proteins were detected diffusely spread in the nucleus within 10 to 12 h and, at these times, nucleocapsids were observed budding from the nucleus. The majority (96%) of these nucleocapsids had no detectable label for tegument and glycoproteins despite the presence of tegument proteins in the nucleus and glycoproteins adjacent to the nuclear membrane. Immunolabeling for tegument proteins and glycoproteins was found abundantly in the cytoplasm of the cell body in multiple discrete vesicular areas: on unenveloped, enveloped, or partially enveloped capsids adjacent to these vesicles and in extracellular virions. These vesicles and intracytoplasmic and extracellular virions also labeled with Golgi markers, giantin, mannosidase II, and TGN38. Treatment with brefeldin A from 2 to 24 h postinfection markedly inhibited incorporation into virions of VP22 and US9 but to a lesser degree with VP16 and VP13/14. These results suggest that, in the cell body of neurons, most tegument proteins are incorporated into unenveloped nucleocapsids prior to envelopment in the Golgi and the *trans*-Golgi network. These findings give further support to the deenvelopment-reenvelopment hypothesis for viral egress. Finally, the addition of tegument proteins to unenveloped nucleocapsids in the cell body allows access to these unenveloped nucleocapsids to one of two pathways: egress through the cell body or transport into the axon.

The tegument is the least understood component of the virion in relation to its structure and function, its role in virus entry, and mechanisms of its assembly and incorporation into virions. The tegument contains at least 19 proteins: VP1/2, VP11/12, VP13/14, VP16, VP22, ICP0, ICP4, the virion shutoff protein (vhs), and the products of genes US9, US10, US11, UL37 (ICP32), UL11, UL13, UL41, and UL 56 (1, 8, 13, 31, 33, 34, 42, 45, 52, 53, 54). A current hypothetical model for the organization of the tegument in alphaherpesviruses suggests that VP1 and the UL37 gene product are present in the deepest layers with VP1 contacting the capsid (10, 20, 34, 36, 55). In pseudorabies virus (PrV), VP11/12 and VP13/14 are suggested to be in the mid-layers, whereas VP22 may be in the most superficial layer interacting with gE/I and gM (27). Two alternative models have been proposed to explain the pathway of maturation of HSV-1 in cell lines. In both models, nucleocapsids acquire an envelope in the inner nuclear membrane. In the first model, these enveloped capsids are transported by vesicular transport from the endoplasmic reticulum (ER) to the cell surface, remaining in the lumenal spaces throughout the entire time. In this model, tegument proteins would be added to the capsids only in the nucleus, before they bud into the inner nuclear membrane (7, 24, 45). The second model involves the

fusion of the enveloped nucleocapsids with the outer nuclear membrane (deenvelopment) and the release of naked nucleocapsids into the cytoplasm. These nucleocapsids undergo a final envelopment (reenvelopment) by budding into a cytoplasmic compartment, such as the Golgi complex, or into cytoplasmic vesicles. In this second model, tegument incorporation could take place either in the nucleus or cytoplasm. This appears to be the mode of envelopment and egress for PrV, varicella-zoster virus, cytomegalovirus, and human herpesvirus 6 (3, 17, 19, 21, 25, 26, 41, 50, 56). There is also increasing evidence for this pathway for herpes simplex virus type 1 (HSV-1) (6, 22, 47, 51).

Identification of the predominant site of tegument protein accumulation and assembly on nucleocapsids may assist in the understanding of the mechanisms of HSV-1 maturation and egress in neurons and other cell types. We have previously shown evidence that HSV-1 is transported in axons in an anterograde direction as unenveloped nucleocapsids coated with some tegument proteins and separately from viral glycoproteins that were found to be within vesicles (23, 37, 40). This suggests that full virion assembly is delayed until the axon terminus. This hypothesis has been supported by recent data showing that the nucleocapsids but not glycoproteins of US9-mutants of PrV are transported anterogradely into axons (5, 49).

In the present study, the distribution and site of assembly of four HSV tegument proteins (VP13/14, VP16, VP22, and US9) and two glycoproteins (gD and gH) in the cell body of rat dorsal root ganglion (DRG) neurons during the first 24 h after

* Corresponding author. Mailing address: Centre for Virus Research, Westmead Millennium Institute, Westmead Hospital/University of Sydney, Westmead, New South Wales 2145, Australia. Phone: (61) 2-9845-9000. Fax: (61) 2-9845-8100. E-mail: tony_cunningham @wmi.usyd.edu.au.

infection was investigated. Further, we sought to identify whether viral particles and free tegument proteins colocalized with Golgi markers. Previously, brefeldin A had been shown to inhibit the anterograde transport into the axons of envelope glycoproteins and most tegument proteins but not nucleocapsids (37). Therefore, the effect of brefeldin A on the tegument protein distribution and viral egress from the cell body was also examined. The findings presented here complement the investigations of axonal transport of capsid, tegument, and glycoproteins by examining the process of HSV maturation and egress in the cell body of neurons. The present study demonstrates that there are similarities in the mechanism of viral egress from the neuronal cell body and cell lines in comparison with the markedly different processes of egress via the axons.

MATERIALS AND METHODS

Cells and virus. A clinical isolate of HSV-1 (CW1) was passaged in HEp-2 cells or in human endothelial fibroblasts (MRC-5) (CSL, Parkville, Australia) and typed with fluorescein-conjugated anti-gC-1 type-specific monoclonal antibody (Syva). Titers were determined in MRC-5 cells by serial 10-fold endpoint dilution as the 50% tissue culture infective dose.

Antibodies to HSV antigens. Antibodies as specified were kindly provided by the following investigators: rabbit polyclonal antibodies to the HSV-1 gD and gH were provided by G. Cohen and R. Eisenberg (University of Pennsylvania, Philadelphia, Pa.) (12), and monoclonal antibody to the HSV tegument protein VP16 (LP1) was provided by A. Minson (University of Cambridge, Cambridge, United Kingdom) (32). Rabbit monospecific antibodies to VP16 and VP22 were provided by P. O'Hare (Marie Curie Institute, Oxted, United Kingdom) (14), rabbit polyclonal to the VP13/14 protein was provided by D. Meredith (University of Leeds, Leeds, United Kingdom) (35), and rabbit polyclonal to the tegument protein US9 was provided by B. Roizman (University of Chicago, Chicago, Ill.) (4).

Antibodies to cellular organelles were provided as follows: rabbit polyclonal antibody to mannosidase II was provided by M. G. Farquhar (University of California San Diego, La Jolla), monoclonal antibodies to giantin were provided by H. P. Hauri (University of Basel, Basel, Switzerland) (28, 46), and sheep anti-rat TGN38 was obtained from Serotec.

The gold (10-nm)-conjugated goat anti-rabbit, anti-mouse, and anti,sheep antibodies were obtained from British Biocell International. The ultrasmall gold-conjugated anti-mouse and anti-rabbit antibodies were purchased from Aurion.

Preparation and culture of dissociated DRG neurons. DRG neurons were prepared from 4-day-old Wistar rat neonates as previously described (37).

HSV-1 infection of neurons. Neurons were exposed to the CW1 clinical isolate of HSV-1 (4.4×10^5 PFU/ml) for 1 h in 16-mm-diameter cluster well plates at multiplicities of infection ranging from 10 to 15 PFU/cell. The inoculum was removed and replaced with fresh Dulbecco modified Eagle medium (DMEM). After infection with HSV-1, neurons were incubated for 6, 8, 10, 12, 17, and 24 h postinfection (hpi) at 37°C under 5% CO_2. The neurons were washed three times in phosphate-buffered saline (PBS) and processed by freeze substitution for transmission immunoelectron microscopy (TIEM). Mock-infected neurons were incubated in DMEM plus 1% fetal calf serum and fixed at 8, 12, and 24 h.

Treatment with inhibitors. Brefeldin A (BFA; Sigma) at a concentration of 1 μg/ml in DMEM was added once at 2 hpi and incubated for 15 or 22 h, before fixation of the neuronal culture.

As controls, neuronal cultures were infected with HSV-1 and then incubated in 1.0 ml of BFA-free medium and fixed at 17 and 24 hpi, respectively.

TIEM. Cultured and HSV-1-infected neurons were processed by TIEM as previously described (37).

Immunolabeling. Tissue sections on Formvar-Pioloform-coated gilded nickel grids were incubated with 5% goat serum for 30 min, washed five times in Tris buffer, and incubated with primary antibody for 3 to 15 h. After five washes in Tris buffer, the sections were incubated for 1 h with the secondary antibody (1:40 dilution) conjugated with either ultrasmall (for dual labeling) or 10-nm gold particles (for single labeling) and washed five times in Tris buffer. For single gold labeling the grids were washed twice in double-distilled water (DDW) and allowed to dry. For double gold labeling, the grids were incubated with 0.1% glutaraldehyde in PBS for 20 min, washed three times in Tris buffer, and washed twice in DDW. The ultrasmall gold particles were silver enhanced by using an EMR-Gent kit (Aurion) for 30 min. The grids were then washed five times in DDW, incubated with 0.05 mM glycine in PBS for 20 min, washed three times, and incubated with a second pair of primary and secondary antibodies (10-nm gold) as described above. For double-labeling experiments, the order of primary antibodies was reversed to avoid any bias due to steric hindrance.

After immunolabeling, the sections were double stained with 1% uranyl acetate in 50% ethanol and Reynolds lead citrate and examined with either a Philips CM10 or BioTWIN transmission electron microscope at 80 and 100 kV.

TEM. Cells were processed as previously described for transmission electron microscopy (TEM) (37).

For TEM and TIEM experiments, results were drawn from two separate experiments in which over 500 cell profiles were examined for each experiment.

RESULTS

The timing of sampling of HSV-1-infected pure cultures of rat neurons for TEM and TIEM was guided by previous kinetic immunofluorescent-confocal microscopic studies examining the appearance and distribution of antigens representing capsid (VP5) tegument (VP16 and VP22) and glycoproteins (gC and gD) (37).

Distribution of HSV-1 tegument proteins in rat DRG neurons. In the present study, the mechanism of tegument acquisition and egress of HSV-1 from the nucleus to the plasma membrane of the cell body was studied by TIEM for the tegument proteins VP13/14, VP16, VP22, and US9 and the glycoproteins gD and gH at 6, 8, 10, 12, 17, and 24 hpi. The intensities of the immunolabeling of viral particles were classified semiquantitatively according to the following criteria: ≤1 gold particle = background, 2 to 3 gold particles = weak, 4 to 6 gold particles = moderate, and ≥7 gold particles = dense.

Distribution of tegument proteins in the nucleus. Neurons infected with HSV-1 at 6 and 8 hpi had no viral particles either within the nucleus or the cytoplasm of the cell body. The ultrastructural morphology of infected neurons was similar to that of uninfected controls, with none of the changes subsequently observed during HSV-1 infection. In addition, no labeling for VP13/14, VP16, VP22, US9, gD, and gH was observed.

At 10 and 12 hpi, the nuclei of infected neurons had undergone ultrastructural changes characteristic of HSV-1 infection, including chromatin dispersal, nucleolus fragmentation, and nuclear membrane convolution (Fig. 1). The nuclei of infected neurons contained numerous viral capsids (mean of 13 capsids per cell section) at 12 hpi and increased in number (mean of 29 capsids per cell section) at 24 hpi. At all times, the number of capsids in the nucleus far exceeded those in the cytoplasm (Tables 1 to 4).

From 10 hpi, there was diffuse but specific labeling for the tegument proteins VP13/14, VP16, VP22, and US9 throughout the nucleoplasm. VP16 label was twofold more abundant than for the other tegument proteins. Labeling for tegument proteins (Fig. 2) and glycoproteins was also observed in small foci along the nuclear membrane (Fig. 3B). A small proportion of intranuclear capsids (3 to 10%) showed weak specific labeling for the tegument proteins VP13/14, VP22, and US9. The proportion of intranuclear capsids labeled weakly to moderately for VP16 was slightly higher (10 to 25%), and this is probably due to the greater abundance of VP16 label in the nucleus (see Fig. 11B and Tables 1 to 4). No labeling for gD and gH was detected within the nucleoplasm or on capsids.

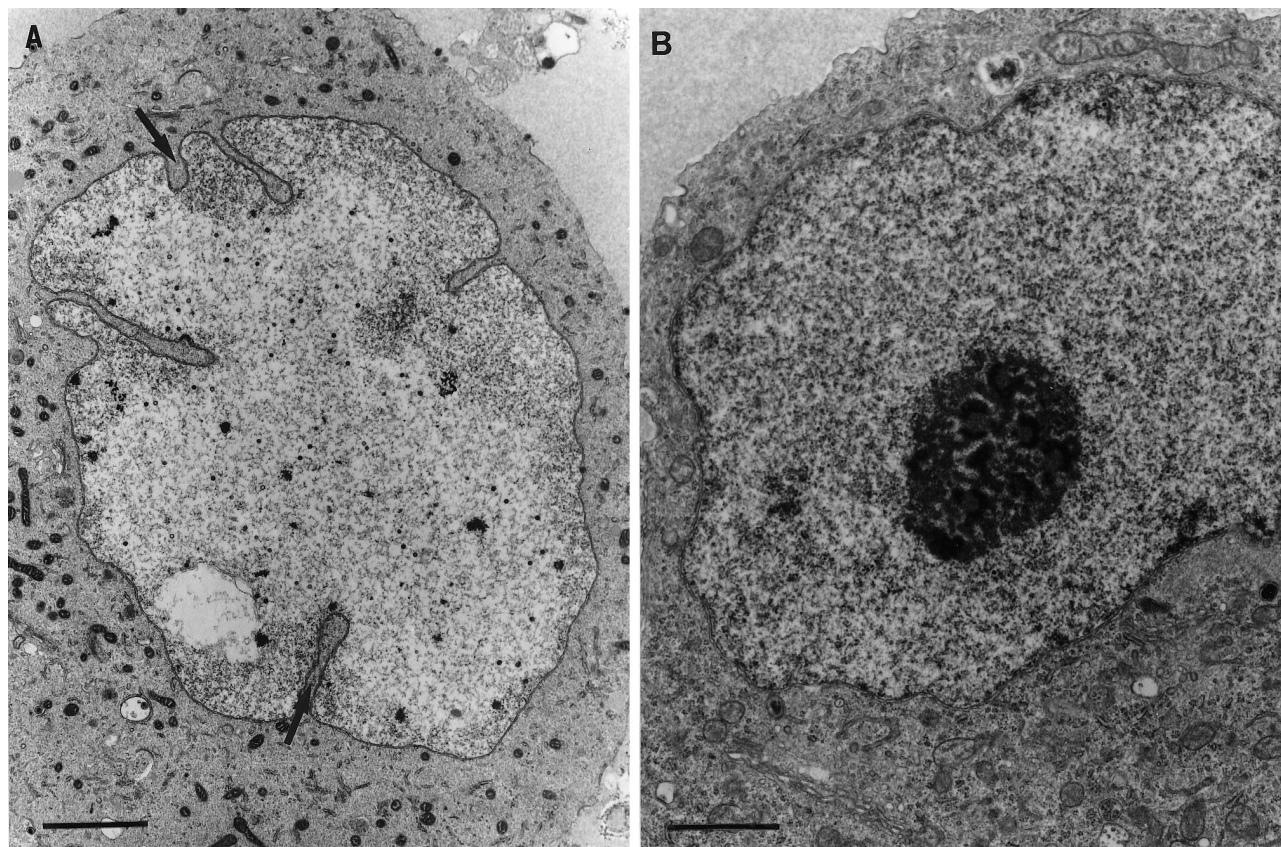Nucleocapsids budding into the cytoplasm were observed in most neurons at 10 and 12 hpi. A key feature during the

FIG. 1. Ultrastructural changes in the nucleus of HSV-1-infected neurons. Nucleolus fragmentation, chromatin dispersal, and nuclear membrane convolution (arrows) are changes that clearly distinguished infected neurons (A) from uninfected neurons (B). Bars, 2 μm.

budding process was that the nuclear membrane contained thick, electron-dense areas surrounding the budding viral particles (Fig. 2 and 3). Most nucleocapsids appeared to bud from these electron-dense areas into the perinuclear space (Fig. 2 and 3A and B; see also Fig. 8A). Some nucleocapsids appeared to protrude through both nuclear membranes (Fig. 3C).

The number of budding viral particles reached its peak at 12 hpi when as many as 47 budding capsids were observed per 22 cells (at a ratio of 2.1 capsids per cell section). Frequently, enveloped nucleocapsids were also observed between the inner and outer nuclear membranes. At 17 and 24 hpi, budding viral particles (three capsids per 22 cells or at a ratio of 0.14 per cell) were also observed but were much less frequent than at 12 hpi.

Usually, the budding viral capsids and the evaginated nuclear membrane did not label for tegument proteins or glycoproteins, even though immunolabel for tegument proteins and glycoproteins was observed along the nuclear membrane (Fig. 2A and 3). Occasional budding particles (2 of 47 capsids counted) showed weak labeling for VP16 and VP13/14 (Fig. 2B). Only nucleocapsids in the cytoplasm, whether enveloped or unenveloped, consistently labeled for tegument proteins (Fig. 3A and C; see also Fig. 5A), and only enveloped capsids labeled for both tegument and glycoproteins (Fig. 4A and B).

Distribution of tegument proteins in the cytoplasm of the cell body. At 6 and 8 hpi, no viral particles were observed in the cytoplasm of the cell body. Furthermore, no labeling for VP13/14, VP16, VP22, and US9 was observed. However, most

TABLE 1. Time course quantitative TIEM analysis of VP13/14 immunolabeling on intranuclear, cytoplasmic, and extracellular HSV-1 capsids at various times postinfection

Time (hpi)	Label intensity	% of capsids $(n)^a$ in:			
		Nucleus	Cytoplasm (unenveloped)	Cytoplasm (enveloped)	Extra-cellular region
12	Total	100 (195)	100 (31)	100 (58)	100 (36)
	Negative	91.5	—	—	—
	Weak	5.6	32.2	—	—
	Moderate	—	35.5	3.5	—
	Dense	—	32.2	96.5	100
17	Total	100 (493)	100 (39)	100 (112)	100 (76)
	Negative	96.8	48.8	6.3	13.2
	Weak	3.2	20.5	10.7	—
	Moderate	—	17.9	13.4	14.5
	Dense	—	12.8	69.6	72.3
24	Total	100 (344)	100 (36)	100 (61)	100 (56)
	Negative	88.7	33.3	—	—
	Weak	11.3	27.8	—	19.6
	Moderate	—	38.9	4.9	—
	Dense	—	—	95.1	80.4
24 (plus BFA)	Total	100 (313)	100 (37)	100 (63)	100 (0)
	Negative	93.0	48.7	22.2	—
	Weak	7.0	51.3	17.5	—
	Moderate	—	—	—	—
	Dense	—	—	60.3	—

^{a} The percentage values shown were derived by counting viral particles in 15 cell profiles for each tegument protein and for each time point. —, Complete absence. n = total number of viral particles.

TABLE 2. Time course quantitative TIEM analysis of VP16 immunolabeling on intranuclear, cytoplasmic, and extracellular HSV-1 capsids at various times postinfection

Time (hpi)	Label intensity	% of capsids (n)[a] in:			
		Nucleus	Cytoplasm (unenveloped)	Cytoplasm (enveloped)	Extra-cellular region
12	Total	100 (212)	100 (34)	100 (61)	100 (58)
	Negative	63.7	5.9	—	—
	Weak	26.9	29.4	—	—
	Moderate	8.5	23.5	—	3.5
	Dense	0.9	41.2	100	96.5
17	Total	100 (480)	100 (68)	100 (123)	100 (103)
	Negative	84.8	44.1	—	—
	Weak	13.3	39.7	7.3	5.8
	Moderate	1.9	11.8	14.7	6.8
	Dense	—	4.4	78.0	87.4
24	Total	100 (470)	100 (123)	100 (76)	100 (129)
	Negative	54.7	1.4	—	—
	Weak	24.5	26.0	4.0	2.3
	Moderate	12.8	23.6	—	—
	Dense	8.0	48.8	96.0	97.7
24 (plus BFA)	Total	100 (403)	100 (144)	100 (84)	100 (0)
	Negative	74.4	39.6	28.6	—
	Weak	20.1	22.2	5.9	—
	Moderate	5.5	20.8	13.1	—
	Dense	—	17.4	52.4	—

[a] See Table 1, footnote a.

TABLE 4. Time course quantitative TIEM analysis of US9 immunolabeling on intranuclear, cytoplasmic, and extracellular HSV-1 capsids at various times postinfection

Time (hpi)	Label intensity	% of capsids (n)[a] in:			
		Nucleus	Cytoplasm (unenveloped)	Cytoplasm (enveloped)	Extra-cellular region
12	Total	100 (201)	100 (18)	100 (51)	100 (54)
	Negative	97.0	—	—	—
	Weak	3.0	22.2	—	—
	Moderate	—	38.9	—	—
	Dense	—	38.9	100	100
17	Total	100 (344)	100 (23)	100 (129)	100 (160)
	Negative	98.3	47.9	1.6	8.2
	Weak	1.7	8.7	5.4	10.0
	Moderate	—	21.7	2.3	10.6
	Dense	—	21.7	90.7	71.2
24	Total	100 (439)	100 (59)	100 (81)	100 (98)
	Negative	96.3	37.3	7.4	3.0
	Weak	3.0	28.8	6.3	4.1
	Moderate	7.0	18.6	16.0	13.3
	Dense	—	15.3	70.3	79.6
24 (plus BFA)	Total	100 (329)	100 (70)	100 (60)	100 (0)
	Negative	97.0	85.7	80.1	—
	Weak	3.0	12.9	16.7	—
	Moderate	—	1.4	1.6	—
	Dense	—	—	1.6	—

[a] See Table 1, footnote a.

neurons showed weak and diffuse labeling for gD and gH throughout the cytoplasm of the cell body. This labeling for glycoproteins was specific to infected neurons and was not detected in uninfected controls.

At 10 and 12 hpi, there was an accumulation of both envel-

TABLE 3. Time course quantitative TIEM analysis of VP22 immunolabeling on intranuclear, cytoplasmic, and extracellular HSV-1 capsids at various times postinfection

Time (hpi)	Label intensity	% of capsids (n)[a] in:			
		Nucleus	Cytoplasm (unenveloped)	Cytoplasm (enveloped)	Extra-cellular region
12	Total	100 (194)	100 (13)	100 (46)	100 (27)
	Negative	92.9	53.8	—	—
	Weak	1.5	30.8	4.4	—
	Moderate	4.1	15.4	15.2	—
	Dense	1.5	—	80.4	100
17	Total	100 (461)	100 (34)	100 (110)	100 (106)
	Negative	94.8	70.6	2.7	5.7
	Weak	5.2	23.5	11.8	7.5
	Moderate	—	5.9	9.1	10.4
	Dense	—	—	76.4	76.4
24	Total	100 (474)	100 (129)	100 (66)	100 (107)
	Negative	87.3	67.4	4.5	—
	Weak	6.8	24.0	7.6	0.9
	Moderate	4.4	6.2	16.7	0.9
	Dense	1.5	2.4	71.2	98.2
24 (plus BFA)	Total	100 (472)	100 (131)	100 (57)	100 (0)
	Negative	87.5	76.1	47.4	—
	Weak	10.0	22.1	45.6	—
	Moderate	2.5	1.5	7.0	—
	Dense	—	—	—	—

[a] See Table 1, footnote a.

oped and unenveloped nucleocapsids in the cytoplasm in clearly defined vesicular areas located mainly in proximity to the nucleus. These areas contained clusters of nucleocapsids that were either enveloped within vesicles or unenveloped within invaginating vesicular membranes, apparently in the process of being enveloped (Fig. 3C and 4A). These areas showed a high density of labeling for both tegument proteins and glycoprotein (Fig. 3C and 4A). The majority of the enveloped nucleocapsids in these areas labeled densely for VP13/14, VP16, VP22, US9, gD, and gH (Fig. 3A and C and Fig. 4A and B), whereas most unenveloped nucleocapsids labeled either weakly or moderately for these tegument proteins (see Fig. 11A and B and Tables 1 to 4).

At 17 and 24 hpi, vesicles containing either one or several enveloped viral particles were observed throughout the cytoplasm. In addition, enveloped as well as unenveloped viral particles were frequently seen in close apposition to Golgi apparatus. The enveloped virions usually labeled densely for tegument proteins (VP13/14, VP16, VP22, and US9) and glycoproteins (gD and gH), similar to the pattern for extracellular virions (Fig. 4C and 5B and C and Tables 1 to 4). However, unenveloped nucleocapsids showed a high variability in the intensity of labeling for each tegument protein (Fig. 5A). At all times, the density of tegument labeling of cytoplasm enveloped was greater than that of cytoplasm unenveloped, followed by the nuclear capsids.

Immunolabel for tegument proteins and glycoproteins was also found on ER and Golgi membranes, cytoplasmic vesicles (empty or enclosing capsids), and plasma membrane (Fig. 3B and 4B and C). Labeling for gD and gH was most intense in Golgi and was moderate on plasma and nuclear membranes (Fig. 4C).
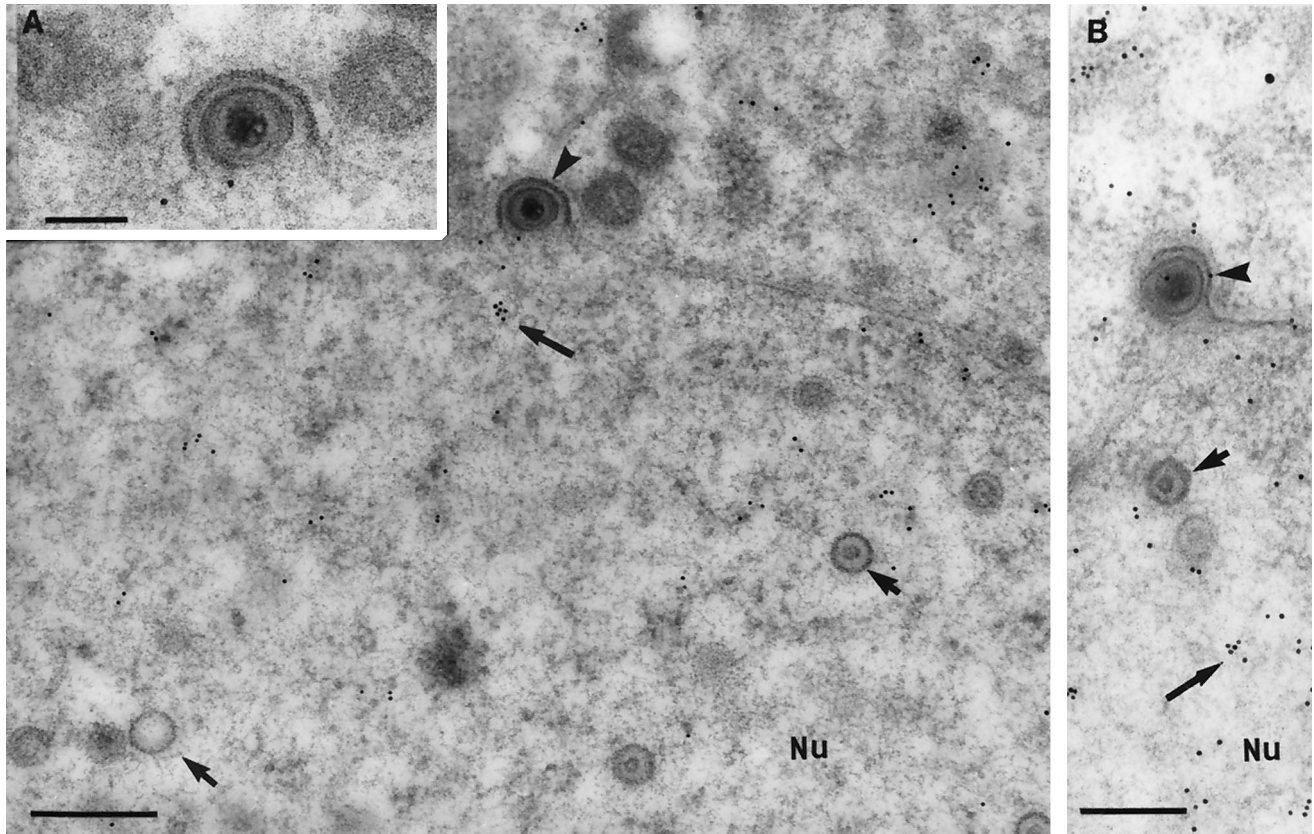
FIG. 2. Immunogold labeling for tegument proteins of HSV-1 nucleocapsids budding through the nuclear membranes (12 hpi). Neurons were embedded in Lowicryl HM20 and reacted with polyclonal antibodies to VP22 (A) or VP13/14 (B). Label for VP22 (A) and VP13/14 (B) (large arrows) was distributed diffusely in the nucleoplasm (Nu) but absent from most intranuclear capsids (small arrows) and budding viral particles (arrowheads). (B) A rare example of a budding viral particle from the nucleus, showing weak labeling for tegument proteins (VP13/14). The inset shows an enlargement of the budding viral particle in panel A. (A) Bar, 300 nm; inset bar, 200 nm. (B) Bar, 200 nm.

At 12 and 17 hpi, generally, more enveloped than unenveloped nucleocapsids were present (at a 2/1 to 3/1 ratio) in the cytoplasm of the cell body of infected neurons. At later stages of infection (24 hpi), the proportion of enveloped to unenveloped viral particles was variable from cell to cell (see Fig. 11A and Tables 1 to 4).

Distribution of tegument proteins on extracellular virions and in axonal processes. At 10 and 12 hpi, no nucleocapsids were observed within axons. Only unenveloped nucleocapsids labeled for VP5 (data not shown) and VP16 (Fig. 5E) were observed in axons at 17 and 24 hpi, a finding consistent with previously published findings by our laboratory (23, 37, 40). Immunolabeling for gD and gH was observed in axons within axonal vesicles at 12, 17, and 24 hpi, and immunolabeling for tegument proteins was observed in vesicles in axons at 17 and 24 hpi (Fig. 5D).

Extracellular enveloped virions were first observed surrounding the cell body at 10 and 12 hpi. These increased in number with time from a mean of 3.0 virions per cell section at 12 hpi to 6.5 at 24 hpi (see Fig. 11A and Tables 1 to 4). At 17 and 24 hpi, extracellular virions were observed not only adjacent to the cell bodies of infected neurons but also adjacent to axonal processes. The vast majority of extracellular viral particles labeled densely for VP13/14, VP16, VP22, US9, gD, and gH (Fig. 5B and C; see also Fig. 11A and Tables 1 to 4).

Identification of organelles colocalizing with viral particles and free tegument antigens. HSV-1-infected neurons were fixed at 12 and 17 hpi and labeled with markers for Golgi complex: giantin (a *cis*-Golgi marker), mannosidase II (a *pan*-Golgi marker), and TGN38 (*trans*-Golgi network [TGN] marker). All Golgi markers consistently colocalized with enveloped particles within vesicles (Fig. 6A, C, and E). Mannosidase II and TGN38 colocalized with unenveloped nucleocapsids close to cytoplasmic vesicles (Fig. 6F). Mannosidase II and TGN38 also consistently colocalized with free tegument proteins (mainly VP13/14 and VP16) within cytoplasmic vesicles (Fig. 6B and D). In addition, all Golgi markers (giantin, mannosidase II, and TGN38) decorated extracellular virions (Fig. 7A, B, and C).

Ultrastructural examination of HSV-1-infected rat DRG neurons. TEM was used to assist in elucidating the possible site(s) of tegument addition and envelopment, especially to better define cellular vesicles, ER, and Golgi. Cells were infected with HSV-1; fixed at 12, 17, and 24 hpi; and processed for conventional TEM by using Spurr resin.

At 12 and 17 hpi, viral particles, whether enveloped or unenveloped, were observed throughout the cytoplasm of the cell body; however, they were localized close to the Golgi (Fig. 8B and C). Unenveloped nucleocapsids were also commonly seen partly surrounded by invaginating vesicles, which were close to
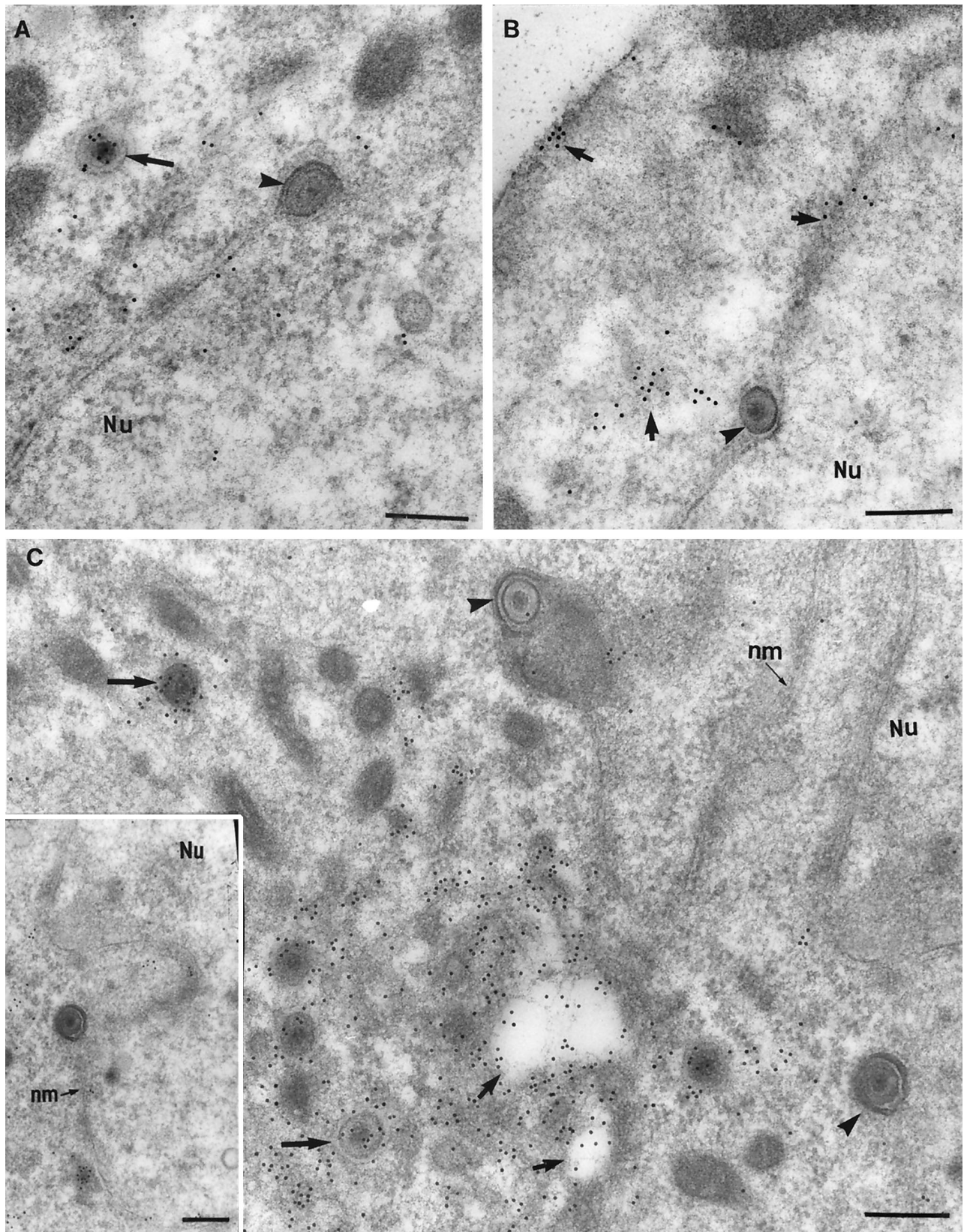
FIG. 3. Comparison of tegument and glycoprotein labeling of budding and cytoplasmic viral particles (12 hpi). Neurons were embedded in Lowicryl HM20 and reacted with polyclonal antibodies against VP22 (A), gD (B), and US9 (C). (A) Unlabeled budding viral particle (arrowhead) and intracytoplasmic enveloped virion (arrow) densely labeled with VP22. Bar, 200 nm. (B) Plasma membrane, cytoplasm, and nuclear membrane (arrows), but not perinuclear enveloped virions (arrowhead) labeled with gD. Bar, 200 nm. (C) Intracytoplasmic enveloped virions (larger arrows) and vesicular regions (smaller arrows) close to the nucleus (Nu) but not the budding virons (arrowheads) labeled densely with US9. Bar, 200 nm. The inset shows a complete view under lower magnification of the virion (at the bottom right corner in Fig. 3C) budding from the nucleus. Bar, 200 nm.
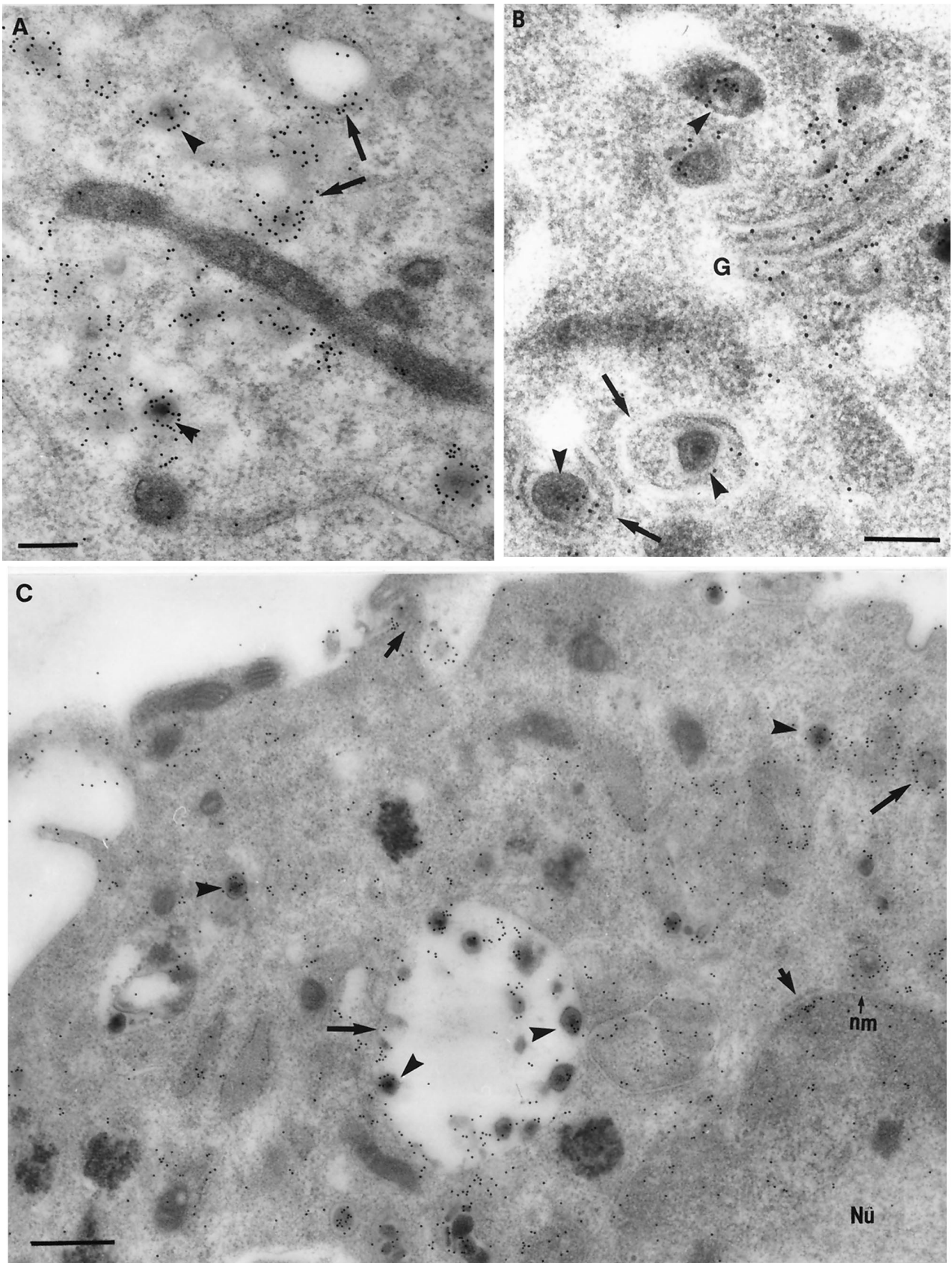
FIG. 4. Immunolabeling of tegument proteins and glycoproteins on viral particles and cytoplasmic membranes in HSV-1-infected neurons. (A) Intracytoplasmic virions (arrowheads) and vesicles (arrows) densely labeled for gD. Bar, 200 nm. (B) Enveloped virions (arrowheads) within vesicles (arrows) and Golgi (G) densely labeled with VP22. Bar, 200 nm. (C) gH labeling of enveloped virions (arrowheads), cytoplasmic vesicles (with or without enclosed virions) (arrows), and nuclear and plasma membranes (small arrows) at 24 hpi. Bar, 500 nm.
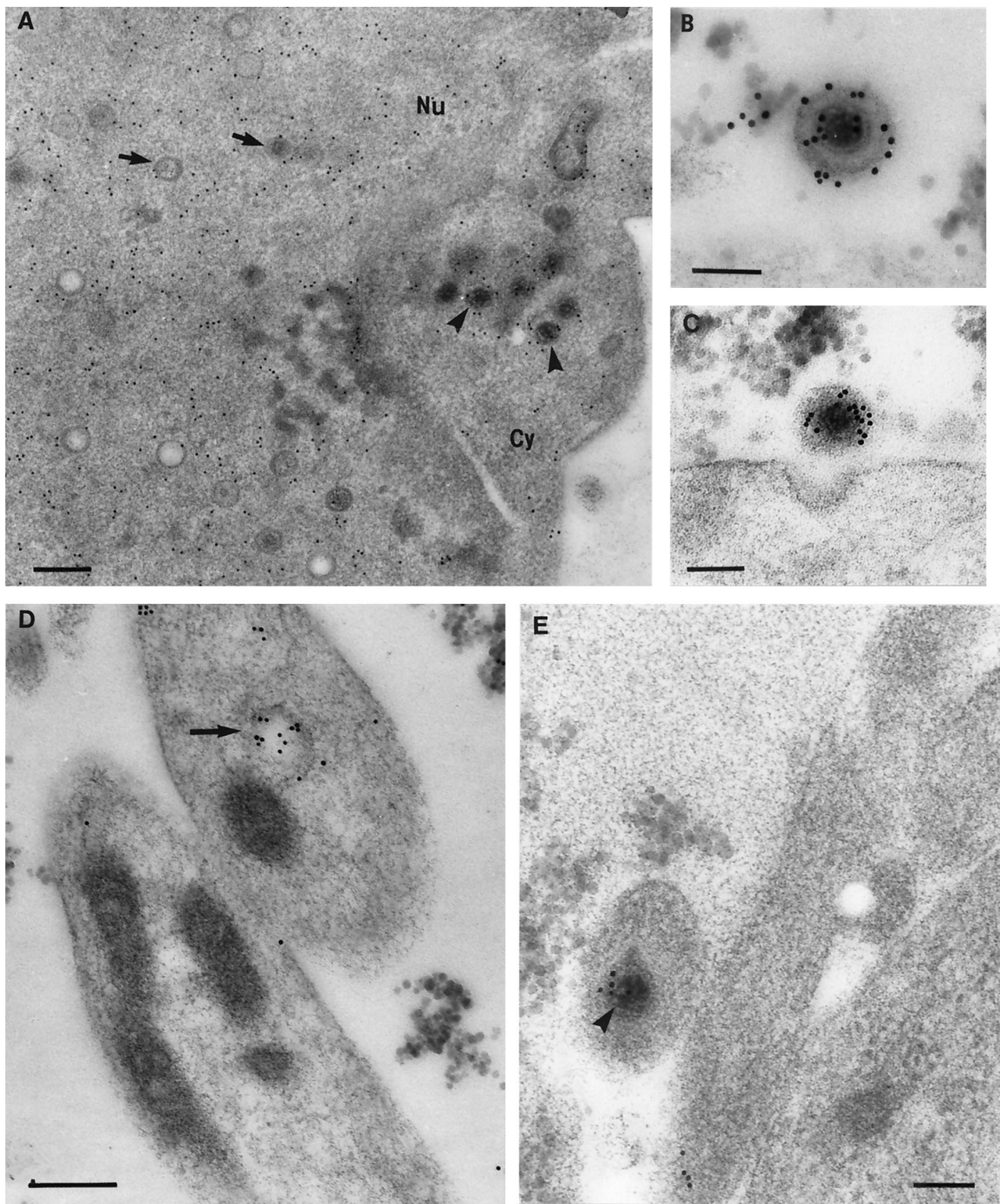
FIG. 5. Immunogold labeling for tegument proteins and glycoproteins on viral particles in the cytoplasm (Cy), extracellular space, and in the axons of HSV-1-infected neurons at 24 hpi. (A) VP16 labeling of the nucleoplasm (Nu), a few intranuclear capsids (arrows), and cytoplasmic unenveloped capsids (arrowheads). Bar, 200 nm. (B and C) Extracellular viral particles densely labeled with VP22 (B) and gD (C). Bars, 100 nm. (D) Axonal vesicles (arrow) decorated with VP16 label. Bar, 200 nm. (E) Unenveloped nucleocapsid (arrowhead) labeled with VP16, within an axonal process. Bar, 100 nm.
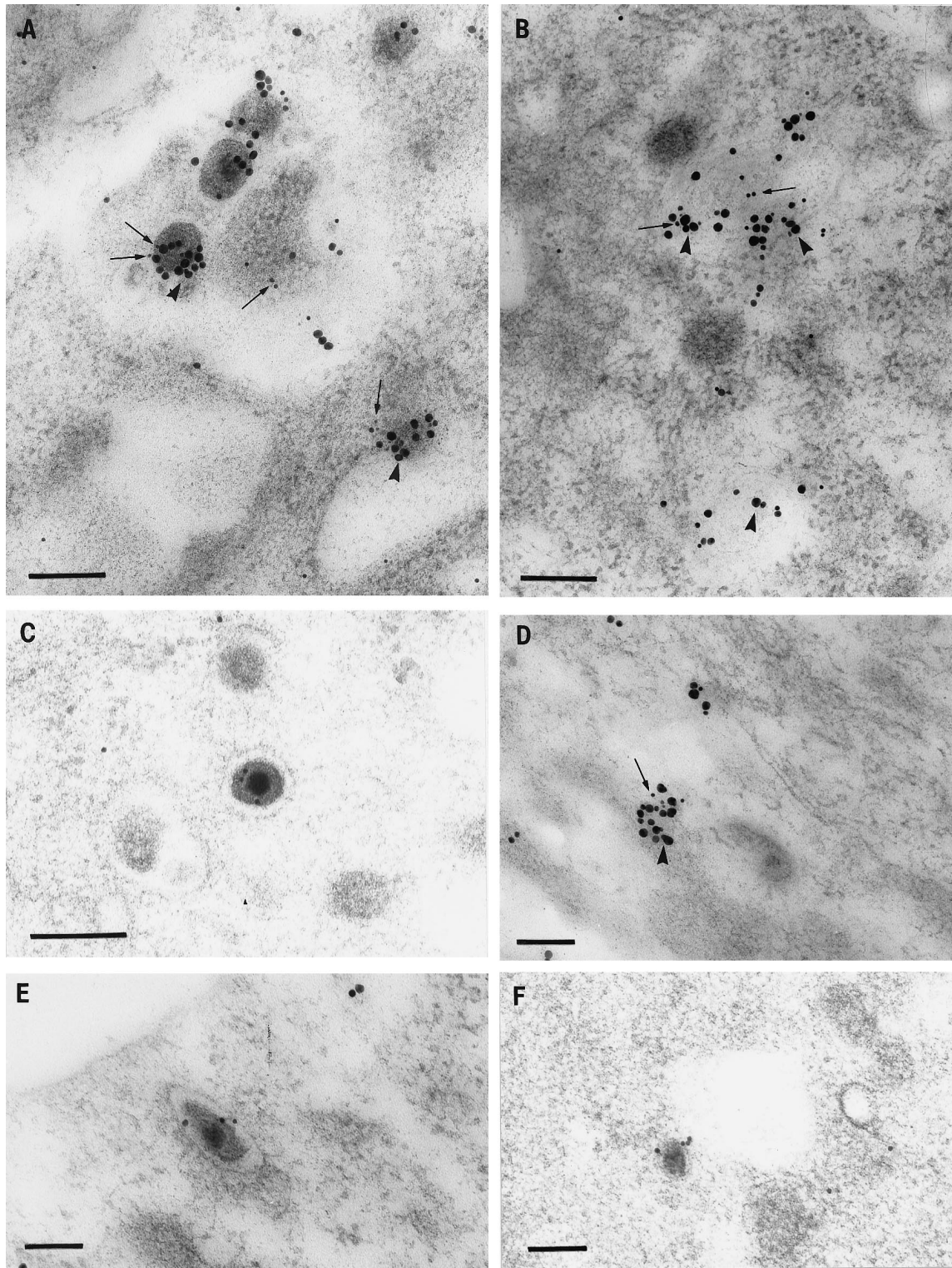
FIG. 6. Immunogold labeling of HSV-1-infected neurons for tegument proteins and Golgi markers. (A) Intracytoplasmic enveloped virions and vesicles double labeled with giantin, indicative of *cis*-Golgi (10-nm gold particles [small arrows]) and VP13/14 (silver-enhanced [SE] gold particles [arrowheads]). Bar, 200 nm. (B) Cytoplasmic vesicles double labeled with mannosidase II, a finding indicative of Golgi (10-nm gold particles [arrows]) and VP16 (SE gold particles [arrowheads]). Bar, 200 nm. (C) Enveloped virion in the cytoplasm labeled with mannosidase II. Bar, 200 nm. (D) Cytoplasmic vesicle doubled labeled with TGN38, indicative of TGN (10-nm gold particles [arrow]) and VP13/14 (SE gold particles [arrowhead]). Bar, 100 nm. (E) Enveloped virion in the cytoplasm labeled with TGN38. Bar, 100 nm. (F) Unenveloped nucleocapsid next to a cytoplasmic vesicle labeled with giantin. Bar, 100 nm.
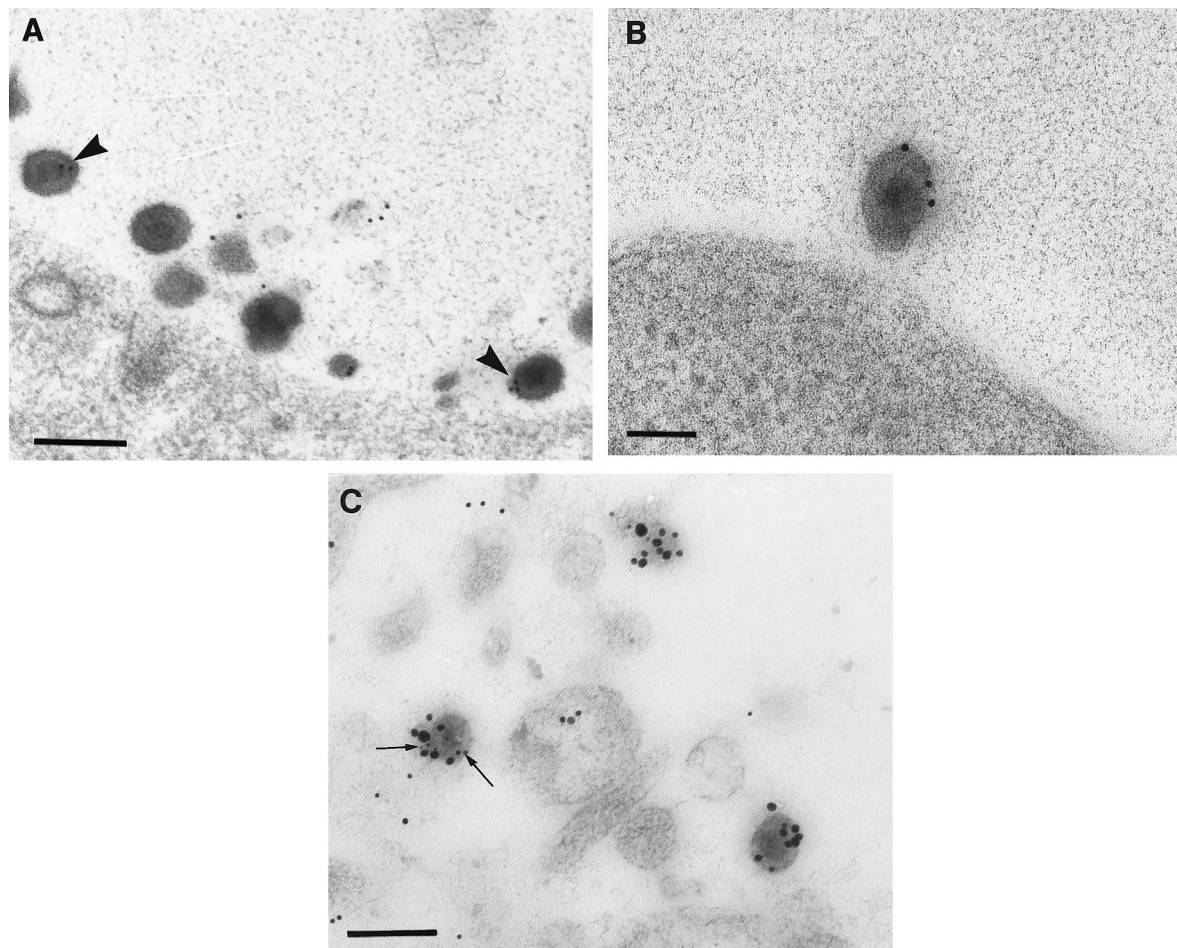
FIG. 7. Immunolabeling with Golgi markers of extracellular HSV-1 particles. (A and B) Extracellular virions labeled with the mannosidase II (arrowheads), which is indicative of Golgi (A), or TNG38, which is indicative of the TGN (B). Bars, 200 nm. (C) Extracellular virions double labeled with giantin, which is indicative of the *cis*-Golgi network (10-nm gold particle [arrows]) and VP13/14 (enhanced gold particles). Bar, 200 nm.

the Golgi (Fig. 8B). In addition, enveloped nucleocapsids within vesicles and unenveloped nucleocapsids partially surrounded by vesicles were also observed close to the cell periphery. Intact Golgi was observed in the cytoplasm of the cell body of infected neurons at all times (Fig. 8B and C). Late in the infection (24 hpi), most viral particles were observed in the extracellular space between neuronal cell bodies and also around axonal processes.

Effects of BFA on the distribution of tegument proteins. To examine the possible involvement of Golgi in the distribution of tegument proteins and the addition of tegument proteins to viral particles in the cytoplasm of the cell body, rat neurons were treated with BFA after infection with HSV-1. The effects of BFA at 17 and 24 hpi were examined by immunolabeling for tegument proteins (VP13/14, VP16, VP22, and US9) and glycoproteins (gD and gH).

Distribution of tegument proteins in the nucleus in the presence of BFA. The nucleus of infected neurons treated with BFA showed numbers of viral capsids (mean of 25 at 24 hpi) similar to those observed in infected controls (without BFA) at 17 and 24 hpi. The characteristic morphological changes associated with HSV-1 infection were also seen in infected neurons treated with BFA. A surprising observation in the nucleus was that chromatin condensed in apposition to the nuclear membrane showed dense labeling for tegument proteins and weak labeling for glycoproteins. This finding was not noted at any time in the absence of BFA.

Immunolabel for VP13/14, VP16, VP22, and US9 was distributed diffusely throughout the nucleoplasm and also in foci along the nuclear membrane. Label for gD and gH was only concentrated at the periphery of the nucleus and also adjacent to the inner and outer nuclear membranes.

At 17 hpi, the perinuclear space was dilated, as well as convoluted in approximately half of the infected neurons treated with BFA. Enveloped nucleocapsids (as many as 52 capsids in 18 cell sections or at a ratio of 3 per cell) were observed to accumulate in this space. The majority of these enveloped nucleocapsids (74%) did not label for tegument proteins (the remaining 26% showed weak labeling) (data not shown). At 24 hpi, there was no longer any accumulation of enveloped viral particles within the perinuclear space as observed at 17 hpi.
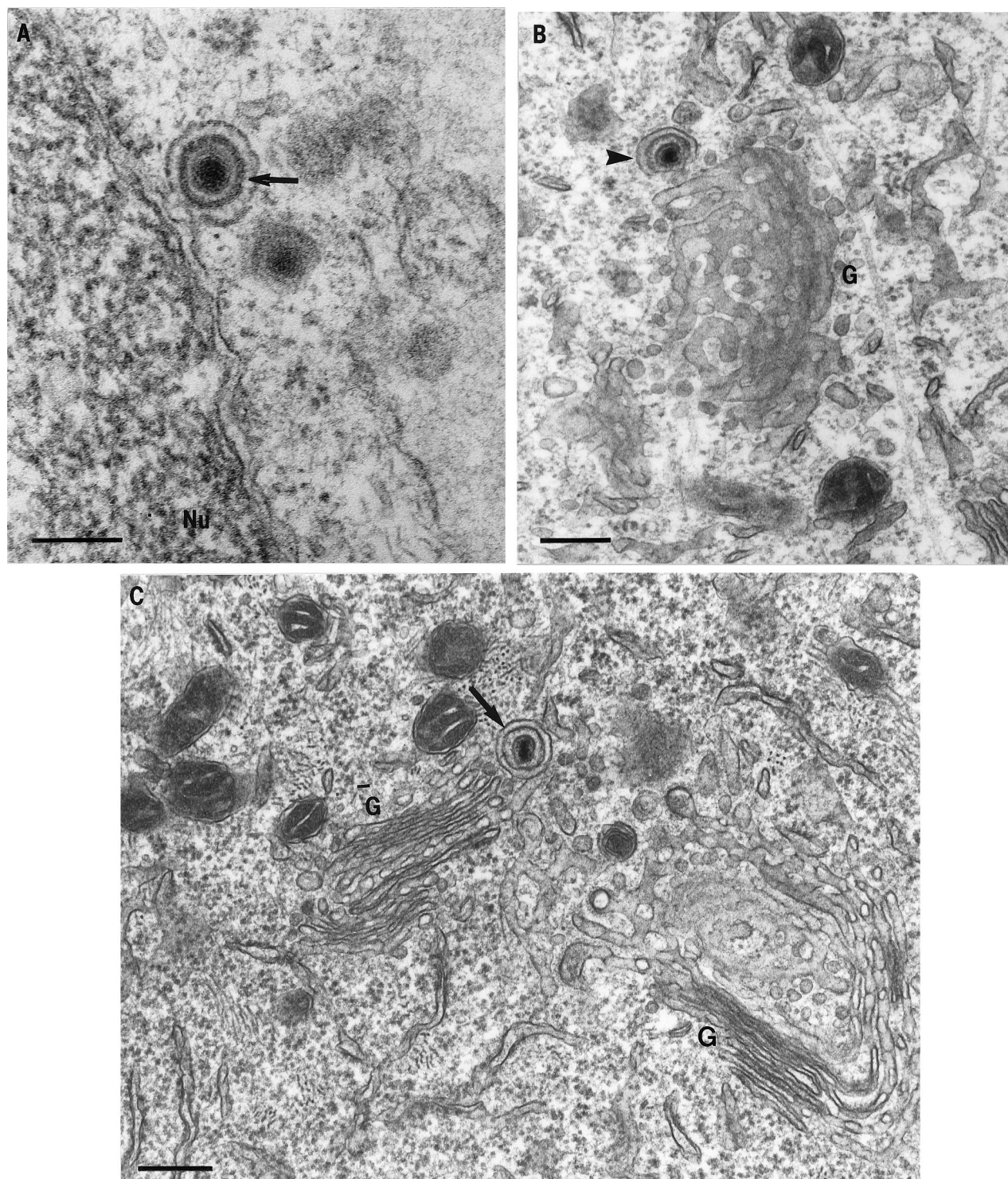
FIG. 8. TEM of HSV-1 particles in the cell body of neurons. (A) An enveloped virion budding through the nuclear membranes (arrow). Bar, 200 nm. Partially enveloped capsid (B) (arrowhead) and enveloped virion within a vesicle (C) (arrow) in close apposition to the Golgi (G). Bars, 300 nm.

Distribution of tegument proteins in the cytoplasm of the cell body. In contrast to untreated cells and as expected, intact Golgi apparatus was not observed in cells treated with BFA. As previously observed, a large proportion of infected neurons contained tubulovesicular structures of various sizes, generally located in close proximity to the nucleus (37). Close examination of these structures revealed that their membranes were in continuity with the nuclear membrane. The composition and mechanism for the formation of these structures is unclear. Only infected neurons treated with BFA but not uninfected or

infected controls contained these tubulovesicular structures at 17 and 24 hpi.

Immunolabel for VP13/14, VP16, VP22, US9, gD, and gH was concentrated on the membrane of these tubulovesicular structures, as well as in vacuoles in the cytoplasm of BFA-treated neurons. However, the distribution of the tegument protein and glycoprotein labeling was altered compared to untreated neurons. Immunolabel for tegument proteins and glycoproteins in BFA-treated neurons was distributed diffusely throughout the cytoplasm, often in association with viral particles and vacuoles, and was not usually observed at the periphery of the cell body. In contrast, in untreated neurons, immunolabeling for tegument proteins and glycoproteins was localized in discrete vesicular areas (Fig. 9 and 10).

Approximately half of the infected neurons treated with BFA at 17 hpi showed viral particles localized to the nucleus and perinuclear space. At this time, mostly enveloped nucleocapsids (at a ratio of 3 to 1 to unenveloped nucleocapsids) accumulated in the cytoplasm in close apposition to the nucleus (data not shown). At 24 hpi, viral particles were mainly present in the cytoplasm in close proximity to the nucleus, and the ratio of enveloped to unenveloped nucleocapsids varied from cell to cell (Fig. 9 and 10 and Tables 1 to 4).

At 17 hpi, labeling for tegument proteins of viral particles decreased significantly compared to untreated controls at the same time. Viral particles (whether enveloped or unenveloped) showed either weak or no labeling. Labeling for glycoproteins of enveloped capsids in close apposition to the nucleus also decreased compared to enveloped capsids in infected untreated controls (Data not shown).

At 24 hpi, labeling of viral particles for tegument proteins was also reduced significantly compared to infected untreated neurons at this time. Most viral particles (enveloped and unenveloped) showed either weak or no labeling for VP22 and US9 (Fig. 9A and 11C). However, labeling for VP13/14 and VP16 was less affected (Tables 1 to 4). The majority of enveloped nucleocapsids labeled moderately to densely for VP13/14 and VP16 (Fig. 9B). However, 37% of the enveloped nucleocapsids showed either weak or no labeling for either protein (Fig. 11C). Thus, BFA partially inhibited VP13/14 and VP16 labeling but markedly inhibited VP22 and US9 labeling. At 24 hpi, labeling for glycoproteins was not significantly reduced by BFA, since most enveloped capsids labeled moderately to densely for gD and gH (Fig. 10).

At later stages of infection (24 hpi), the proportion of enveloped to unenveloped nucleocapsids varied from cell to cell, as it did in infected untreated neurons. Unenveloped nucleocapsids in the perinuclear areas showed weak labeling for all tegument proteins, but those close to the cell periphery did not label for any tegument proteins.

Distribution of tegument proteins in axonal processes. No labeling for VP13/14, VP16, VP22, US9, gD, and gH in vesicles was observed within axonal processes. Only unenveloped nucleocapsids labeled for VP5 were observed in the presence of BFA at 17 and 24 hpi, as previously described (37). No viral particles were observed in the extracellular space surrounding neuronal cell bodies or close to axonal processes compared to infected neurons (untreated) at 17 and 24 hpi.

Uninfected (BFA-untreated) cell controls. Mock-infected neurons did not show any morphological changes characteristic of HSV-1 infection. Intact Golgi and no tubulovesicular structures were observed in the cytoplasm of the cell body. No immunolabeling for tegument proteins or glycoproteins was detected at any time.

DISCUSSION

In the present study, the mechanism of HSV-1 tegument acquisition and viral egress from the cell body of HSV-1-infected rat DRG neurons was investigated by TEM and TIEM. The distribution of multiple tegument proteins (VP13/14, VP16, VP22, and US9) and two envelope glycoproteins (gD and gH) was first analyzed at various times ranging from 6 to 24 hpi. Then, the effect of BFA on the tegument acquisition and the colocalization of viral particles and free tegument protein with Golgi markers was examined. These times were guided by previous confocal microscopy studies (37).

We show here that HSV-1 tegument is mainly acquired in neurons in a cytoplasmic compartment. A key finding is that the vast majority of nucleocapsids (95%) budding out of the nucleus did not label for tegument proteins VP13/14, VP16, VP22, and US9 even though immunolabel for tegument proteins was consistently observed in the nucleus and in small foci in proximity to the nuclear membrane. Thus, these results show that the great majority of nucleocapsids budding out of the nucleus either do not contain VP13/14, VP16, VP22, or US9 or that these tegument proteins are present at low levels that limit their detection by conventional techniques.

From the early stages of HSV-1 replication, there was a diffuse pattern of labeling of all tegument proteins throughout the nucleoplasm, and there were also small foci of label in close association with the nuclear membranes. Viral capsids within the nucleus occasionally labeled weakly for tegument proteins. With the exception of VP16, moderate to dense labeling for tegument proteins on nucleocapsids was restricted to viral particles in the cytoplasm of the cell body or extracellular virions. The large amount of diffuse label for VP16 in the nucleus may result in the apparent labeling of capsids; this does not occur when the capsids bud into the perinuclear space (as with the other tegument proteins).

The presence of tegument proteins within the nucleus may reflect a nonstructural role. For instance, VP16 transactivates the transcription of the α genes and has been shown to localize to the nucleus during HSV infection (38, 45). Previous reports of VP22 distribution in cell lines have differed in their capacity to detect VP22 in the nucleus, which may reflect technical differences in fixation and/or the functional and structural heterogeneity of VP22 (2, 15, 16). Our data are in agreement with these observations since differences in VP22 distribution were seen both by confocal microscopy and TIEM (data not shown).

Exit of viral capsids from the nucleus occurred by budding from electron-dense areas in the nuclear membrane into the perinuclear space. Nucleocapsids protruding through both nuclear membranes were also observed here and have also been commonly observed with PrV (21, 22). This could represent a second pathway of nuclear egress (21, 22).

Surprisingly, nucleocapsids budding out of the nucleus did not label for the envelope glycoproteins gD and gH. The reasons why glycoproteins are observed in the nuclear membranes but not in budding nucleocapsids or on those in the perinuclear
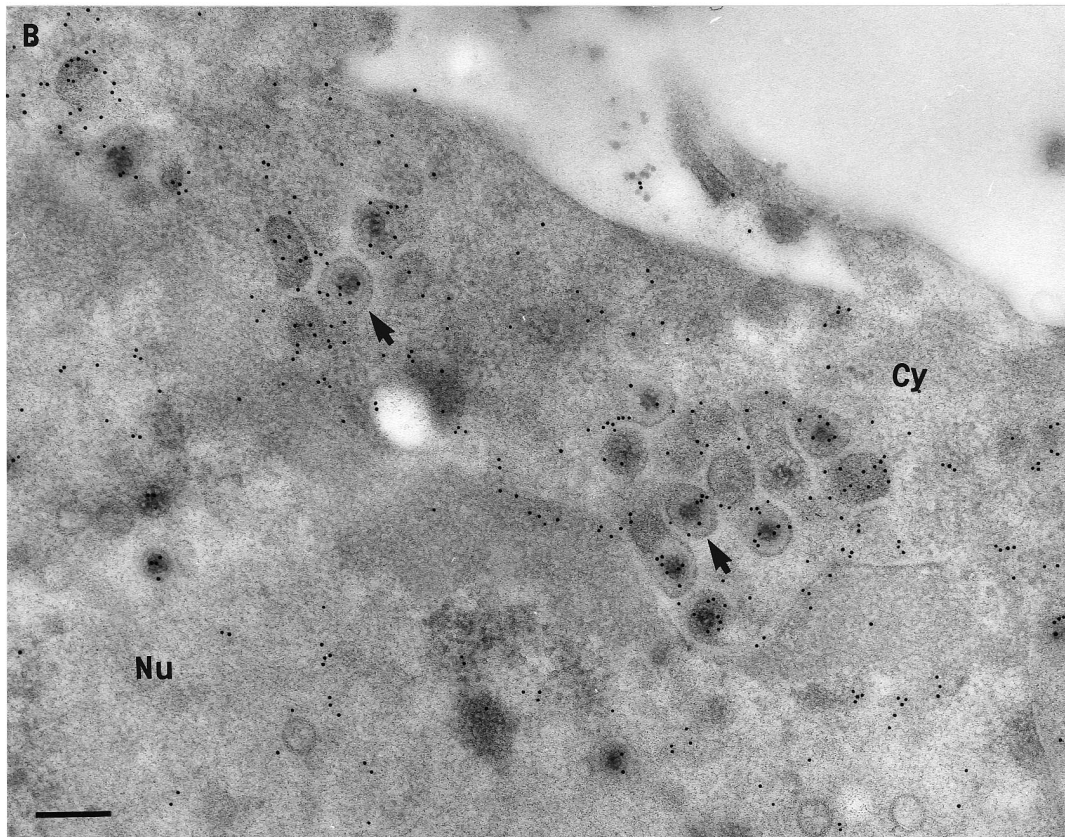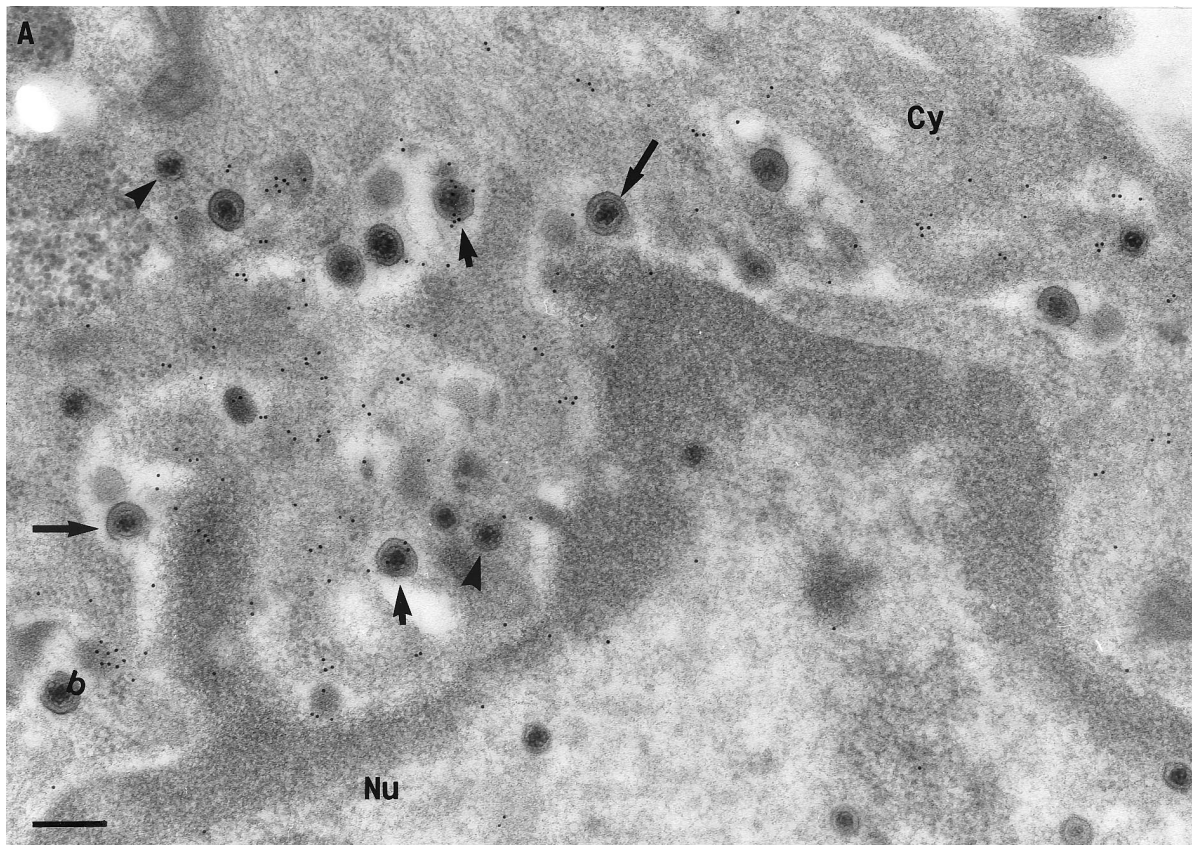
FIG. 9. Immunogold labeling for tegument proteins of HSV-1-infected neurons treated with BFA. (A) BFA greatly inhibited the incorporation of US9 into enveloped (large arrows) and unenveloped viral particles (arrowheads) of US9, as shown by the weak or dense (small arrows) or no labeling of viral particles for US9 (large arrows). Bar, 200 nm. (B) VP13/14 incorporation was less markedly inhibited, since most enveloped virions (arrows) labeled densely with VP13/14. Bar, 200 nm.
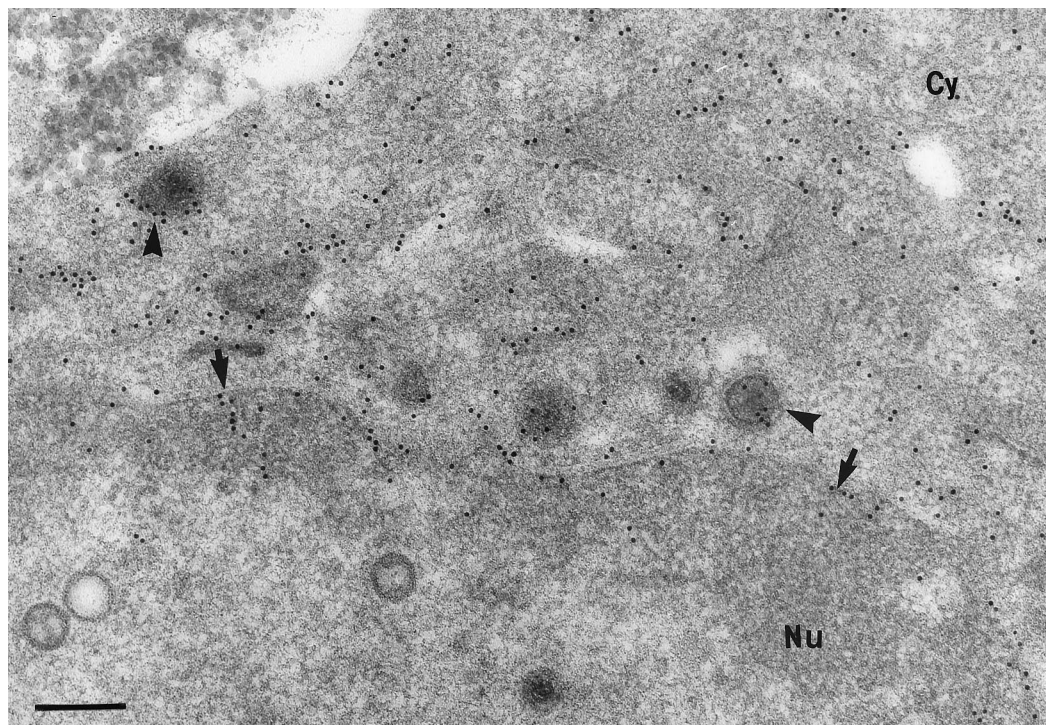
FIG. 10. Immunogold labeling for gH of HSV-1-infected neurons treated with BFA. Label for gH is present along the nuclear membrane (arrows), throughout the cytoplasm of the cell body, and on enveloped virions (arrowheads). Bar, 200 nm.

space, except after treatment with BFA, remain unclear. Perhaps the marked changes induced in the nuclear membrane by BFA allow lateral entry of gD into the budding virion from the adjacent inner nuclear membrane. In support of our findings, Granzow et al. reported that, in cells infected with PrV deleted of gB and gH, there was normal viral assembly and maturation in the cytoplasm, indicating that gB and gH are not required in nuclear budding (22). The electron-dense areas within the inner nuclear membrane at the site of nucleocapsid budding are supposedly aggregations of viral proteins (45). However, in our study no labeling for gD and gH was observed in these areas. Further examination of these electron-dense areas for other envelope glycoproteins and other tegument proteins such as UL34 (26) are needed.

After budding from the nucleus, viral particles acquired tegument proteins and an envelope in the cytoplasm of the cell body, with most tegument-labeled nucleocapsids, enveloped or unenveloped, localizing to discrete vesicular regions in the cytoplasm. These regions also had the highest concentration of immunolabel for tegument proteins and glycoproteins. These vesicular regions labeled with Golgi markers, giantin (a *cis*-Golgi marker), mannosidase II (a *pan*-Golgi marker), and TGN38 (a TGN marker). Moreover, TEM studies showed that numerous enveloped or unenveloped nucleocapsids and apparently enveloping nucleocapsids lay adjacent to the Golgi. Thus, Golgi and the TGN appear to be the sites for addition of tegument proteins to nucleocapsids and of secondary envelopment for HSV-1 in rat DRG neurons. In addition, extracellular and cytoplasmic enveloped nucleocapsids (within vesicles) also labeled for markers of Golgi and TGN, indicating that the final viral envelope was at least partly derived from these organelles.

Our findings show that HSV-1 tegument is mainly acquired in a cytoplasmic compartment in neurons. These results build on previous TEM studies in cell lines which showed suggestive evidence for the addition of tegument proteins in the cytoplasm based on the thickness of the tegument (22, 44). For example, comparative studies of alpha- and betaherpesviruses have shown that the tegument of cytoplasmic and extracellular herpesviruses is larger and less electron dense than particles in the perinuclear space (i.e., a thinner "primary" and a thicker "secondary" tegument (21, 56).

The present study also provides further evidence to support the model proposed by Stackpole (48), in which nucleocapsids are deenveloped at the outer nuclear membrane and reenveloped in the cytoplasm. Our observation that budding viral particles do not usually label for the tegument proteins implies that after an initial envelopment at the inner nuclear membrane, nucleocapsids must deenvelop in the cytoplasm in order to acquire tegument proteins. The observations that both enveloped and unenveloped nucleocapsids in the cytoplasm in close proximity to the nucleus label with tegument proteins and the higher proportion of enveloped virions at early times suggest that tegument protein acquisition, followed by reenvelopment, occurs rapidly after budding into the cytoplasm. Furthermore, the colocalization of Golgi and TGN markers with viral particles and free tegument proteins provides evidence that the Golgi and the TGN are the sites of secondary envelopment of HSV-1 in neurons. This is consistent with reports that the Golgi and TGN also appear to be the sites of final envelopment for PrV and varicella-zoster virus (19, 21, 56).

Some of the most convincing evidence for the deenvelopment/reenvelopment pathway of egress has been reported by
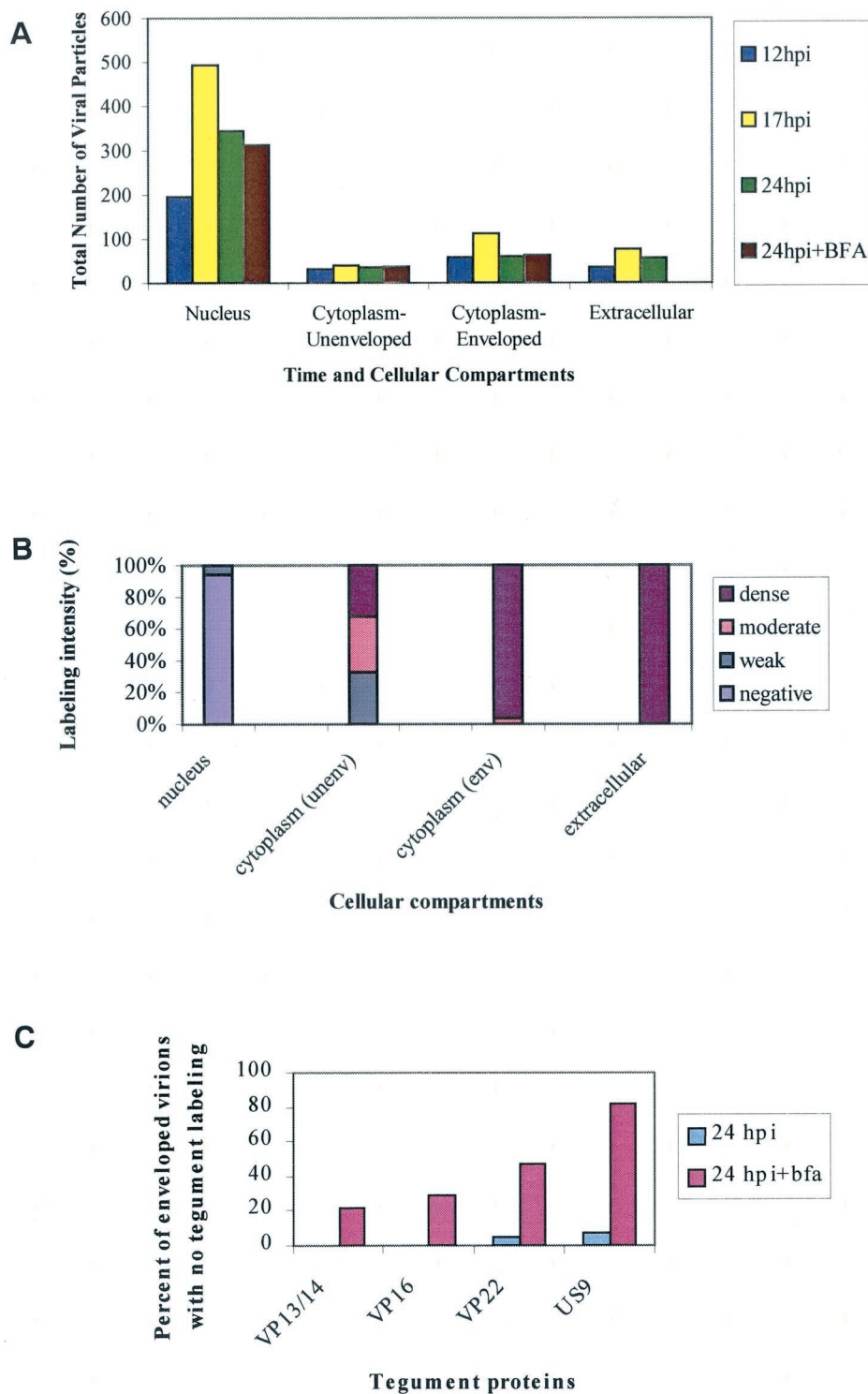
FIG. 11. Quantitative TIEM analysis of tegument proteins immunolabeling on HSV-1 capsids at various times postinfection. (A) Total numbers of viral particles in the nucleus, cytoplasm, and extracellular milieu at various times after HSV-1 infection with or without BFA. (B) Percent labeling intensity for VP13/14 on HSV-1 capsids in the nucleus, cytoplasm, and extracellular milieu at 12 hpi. (C) Percent of enveloped virions in the cytoplasm of the cell body lacking tegument protein labeling at 24 hpi with or without BFA. The values shown were derived by counting the number of viral particles in 15 cell profiles for each tegument protein at each time point.
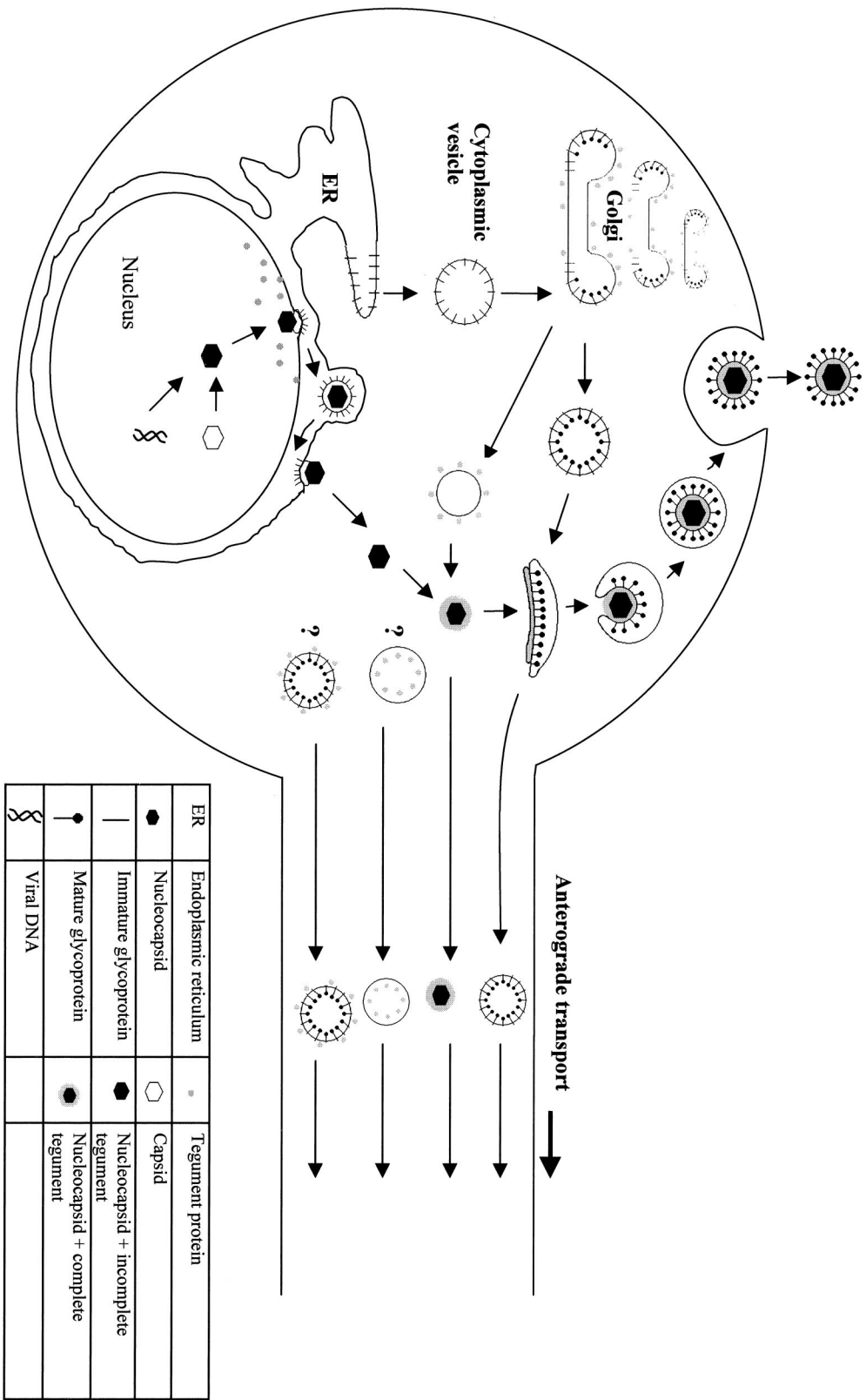
FIG. 12. Proposed model of assembly and egress of HSV-1 in the cell body of (rat) DRG neurons.

Klupp et al., who showed that the product of UL34 gene of PrV is present on enveloped virions in the perinuclear space but is undetectable in intracytoplasmic and extracellular enveloped virions. However, the tegument protein UL49 (VP22) is present in mature enveloped virions but absent from enveloped virions in the perinuclear space (26). Furthermore, Skepper et al. demonstrated that in cells infected with HSV-1 encoding a gD, which is retrieved to the ER, gD was present only in perinuclear enveloped virions and absent in mature progeny virions (47). Our observations of glycoprotein distribution differ from those of Skepper et al., who observed approximately equal labeling densities for gD in perinuclear and extracellular virions and little labeling of plasma membranes compared to nuclear and cytoplasmic membranes (47). In the present study, the most intense staining was on extracellular or cytoplasmic enveloped virions, and cytoplasmic membranes labeled more intensely than either plasma or nuclear membranes. This difference in distribution of gD observed between these two studies could be attributed either to biological differences between BL1 cells and primary neurons or possibly to technical variations.

The consistently denser labeling for all tegument proteins in enveloped compared with unenveloped nucleocapsids could be explained by tegument proteins being added initially to the capsid adjacent to the Golgi and then secondarily at the time of envelopment in the Golgi and TGN. The latter is supported by the localization of both tegument proteins and glycoproteins in the Golgi and TGN. The relatively similar proportions of unenveloped nucleocapsids unlabeled for each tegument protein in the cytoplasm at 12, 17, and 24 h could be explained by a continuing flow from the nucleus (which has a much higher proportion of capsids at all times) and/or a constant proportion of unenveloped capsids to which tegument is never added.

BFA treatment of HSV-1-infected rat DRG neurons inhibited the egress of HSV-1 and resulted in the accumulation of mostly enveloped nucleocapsids in the cell body of infected neurons, as previously described (37). Enveloped virions accumulated first in the space between inner and outer nuclear membranes and subsequently in the cytoplasm but failed to be transported to the extracellular space. This result is consistent with previous studies in cell lines (although in some studies, BFA was added for shorter periods) (9, 11). BFA inhibited the incorporation into enveloped nucleocapsids of most VP22 and US9, as shown by decreased immunolabeling. However, the addition of VP16 and VP13/14 was less markedly inhibited by BFA. BFA causes cell organelles to collapse into isolated and functional organelle systems, such as ER with Golgi and TGN with endosomes and plasma membrane. The Golgi and ER membranes fuse, thereby ablating Golgi structure and inhibiting its function (18, 29, 30, 39, 43). Transport within these organelle systems continues, but transport to and from these systems is blocked by BFA (30). The dissociation between the two systems may explain the accumulation of enveloped virions in the cytoplasm and the lack of extracellular virions. Hence, in the presence of BFA, secondary envelopment occurred in the ER-Golgi compartment. The inhibition of addition of VP22, US9, and most VP13/14 and VP16 to capsids is consistent with a major role for TGN in tegument protein assembly. Our findings show that VP16 and VP13/14 may be not only added to nucleocapsids undergoing secondary envelopment in the

TGN but also directly to unenveloped nucleocapsids at a slightly earlier stage (Golgi). The addition of the more superficial VP22 may occur predominantly in the TGN. In PrV, US9 is a type II membrane protein that is incorporated into the virion membrane in the TGN (5). The distribution of US9 in neurons noted in the present study was very similar to that of VP22, especially after BFA treatment. This is consistent with a role in late viral assembly and possibly in glycoprotein transport in the axon, as with PrV (49). Future studies with other tegument proteins are needed to confirm these findings and should focus on the interactions between outer capsid proteins, tegument proteins, and glycoproteins in the Golgi and TGN and their role in envelopment. The mechanisms of transport of free tegument protein in vesicles into the axon (and whether they are associated with glycoproteins) also needs further investigation (Fig. 12).

The key findings presented in the present study are that HSV-1 tegument addition occurs primarily in the cytoplasm of the neuronal cell body and that the major sites are the vesicles of the Golgi and TGN. These results provide further evidence that unenveloped nucleocapsids with tegument proteins on their surface are functional in the cytoplasm around the nucleus of neurons. Hence, unenveloped nucleocapsids can either be transported to the axon hillock and then along microtubules in the axons to its terminus or be reenveloped in the Golgi to exit from the cell body. Overall, our findings suggest that HSV-1 has evolved two different mechanisms for its transport and egress from DRG neurons that are specific for exit either from the axons or the cell body (Fig. 12).

ACKNOWLEDGMENTS

We thank Carol Robinson, Levina Dear, and Mary Simonian for assistance with electron microscopy and photographic work. We thank Claire Wolczak and Brenda Wilson for secretarial assistance. We also thank Mary-Ann Lau for assistance with Fig. 11 and 12.

This work was supported by Australian National Health and Medical Research Council project grant 700738.

REFERENCES

1. **Baines, J. D., and B. Roizman.** 1992. The UL11 gene of herpes simplex virus 1 encodes a function that facilitates nucleocapsid envelopment and egress from cells. J. Virol. **66:**5168–5174.
2. **Blouin, A., and J. A. Blaho.** 2001. Assessment of the subcellular localization of the herpes simplex virus structural protein VP22 in the absence of other viral gene products. Virus Res. **81:**57–68.
3. **Brack, A. R., J. M. Dijkstra, H. Granzow, B. G. Klupp, and T. C. Mettenleiter.** 1999. Inhibition of virion maturation by simultaneous deletion of glycoproteins E, I, and M of pseudorabies virus. J. Virol. **73:**5364–5372.
4. **Brandimarti, R., and B. Roizman.** 1997. US9, a stable lysine-less herpes simplex virus 1 protein, is ubiquinated before packaging into virions and associated with proteosomes. Proc. Natl. Acad. Sci. USA **94:**13973–13978.
5. **Brideau, A. D., J. P. Card, and L. W. Enquist.** 2000. Role of pseudorabies virus US9, a type II membrane protein, in infection of tissue culture cells and the rat nervous system. J. Virol. **74:**834–845.
6. **Browne, H., S. Bell, T. Minson, and D. W. Wilson.** 1996. An endoplasmic reticulum-retained herpes simplex virus glycoprotein H is absent from secreted virions: evidence for reenvelopment during egress. J. Virol. **70:**4311–4316.
7. **Campadelli-Fiume, G., F. Farabegoli, S. Di Gaeta, and B. Roizman.** 1991. Origin of unenveloped capsids in the cytoplasm of cells infected with herpes simplex virus. J. Virol. **65:**1589–1595.
8. **Campbell, M. E. M., J. W. Palfreyman, and C. M. Preston.** 1984. Identification of herpes simplex virus DNA sequences which encode a *trans*-acting polypeptide responsible for stimulation of immediate-early transcription. J. Mol. Bol. **180:**1–19.
9. **Chatterjee, S., and S. Sarkar.** 1992. Studies on endoplasmic reticulum-Golgi complex cycling pathway in herpes simplex virus-infected and brefeldin A treated human fibroblast cells. Virology **191:**327–337.
10. **Chen, D. H., H. Jiang, M. Lee, F. Liu, and Z. H. Zhou.** 1999. Three dimen-

sional visualization of tegument/capsid interaction in the intact human cytomegalovirus. Virology **260**:10–16.

11. **Cheung, P., B. W. Banfield, and F. Tufaro.** 1991. Brefeldin A arrests the maturation and egress of herpes simplex virus particles during infection. J. Virol. **65**:1893–1904.

12. **Cohen, G. H., M. Ponce de Leon, H. Diggelmann, W. C. Lawrence, R. J. Vernon, and R. J. Eisenberg.** 1980. Structural analysis of the capsid polypeptides of herpes simplex virus types 1 and 2. J. Virol. **34**:521–531.

13. **Elliott, G. D., and D. M. Meredith.** 1992. The herpes simplex virus type 1 tegument protein VP22 is encoded by gene UL49. J. Gen. Virol. **73**:723–726.

14. **Elliott, G., G. Mouzakitis, and P. O'Hare.** 1995. VP16 interacts via its activation domain with VP22, a tegument protein of herpes simplex virus, and is relocated to a novel macromolecular assembly in coexpressing cells. J. Virol. **69**:7932–7941.

15. **Elliott, G., and P. O'Hare.** 1999. Live-cell analysis of a green fluorescent protein-tagged herpes simplex virus infection. J. Virol. **73**:4110–4119.

16. **Elliott, G., and P. O'Hare.** 2000. Cytoplasm-to-nucleus translocation of a herpesvirus tegument protein during cell division. J. Virol. **74**:2131–2141.

17. **Enquist, L. W., P. J. Husak, B. W. Banfield, and G. A. Smith.** 1999. Infection and spread of alphaherpesviruses in the nervous system. Adv. Virus Res. **51**:237–347.

18. **Fujiwara, T., K. Oda, S. Yokota, A. Takatsuki, and Y. Ikehara.** 1988. Brefeldin A causes disassembly of the Golgi complex and accumulation of secretory proteins in the endoplasmic reticulum. J. Biol. Chem. **263**:18545–18552.

19. **Gershon, A. A., D. L. Sherman, Z. Zhu, C. A. Gabel, R. T. Ambron, and M. D. Gershon.** 1994. Intracellular transport of newly synthesized varicella-zoster virus: final envelopment in the *trans*-Golgi network. J. Virol. **68**:6372–6390.

20. **Gibson, W.** 1996. Structure and assembly of the virion. Intervirology **39**:389–400.

21. **Granzow, H., F. Weiland, A. Jons, B. G. Klupp, A. Karger, and T. C. Mettenleiter.** 1997. Ultrastructural analysis of the replication cycle of pseudorabies virus in cell culture: a reassessment. J. Virol. **71**:2072–2082.

22. **Granzow, H., B. G. Klupp, W. Fuchs, J. Veits, M. Osterrieder, and T. C. Mettenleiter.** 2001. Egress of alphaherpesviruses: comparative ultrastructural study. J. Virol. **75**:3675–3684.

23. **Holland, D. J., M. Miranda-Saksena, R. A. Boadle, P. Armati, and A. L. Cunningham.** 1999. Anterograde transport of herpes simplex virus proteins in axons of peripheral human fetal neurons: an immunoelectron microscopy study. J. Virol. **73**:8503–8511.

24. **Johnson, D. C., and P. G. Spear.** 1982. Monensin inhibits the processing of herpes simplex virus glycoproteins, their transport to the cell surface, and the egress of virions from infected cells. J. Virol. **43**:1102–1112.

25. **Jones, F., and C. Grose.** 1988. Role of cytoplasmic vacuoles in varicella-zoster virus glycoprotein trafficking and virion envelopment. J. Virol. **62**:2701–2711.

26. **Klupp, B. G., H. Granzow, and T. C. Mettenleiter.** 2000. Primary envelopment of pseudorabies virus at the nuclear membrane requires the UL34 gene product. J. Virol. **74**:10063–10073.

27. **Klupp, B. G., H. Granzow, E. Mundt, and T. C. Mettenleiter.** 2001. Pseudorabies virus UL37 gene product is involved in secondary envelopment. J. Virol. **75**:8927–8936.

28. **Lindstedt, A. D., M. Foguet, M. Renz, H. P. Seelig, B. S. Glick, and H.-P. Hauri.** 1995. A C-terminally anchored Golgi protein is inserted into the endoplasmic reticulum and then transported to the Golgi apparatus. Proc. Natl. Acad. Sci. USA **92**:5102–5105.

29. **Lippincott-Schwartz, J., L. C, Yuan, J. S. Bonifacino, and R. D. Klausner.** 1989. Rapid redistribution of Golgi proteins into the ER in cells treated with brefeldin A: evidence for membrane cycling from Golgi to ER. Cell **56**:801–813.

30. **Lippincott-Schwartz, J., Yuan, L. C. Bonifacino, and R. D. Klausner.** 1991. Brefeldin A's effects on endosomes, lysosomes, and the TGN suggest a general mechanism for regulating organelle structure and membrane traffic. Cell **67**:601–616.

31. **McLauchlan, J., and F. J. Rixon.** 1992. Characterization of enveloped tegument structures (L particles) produced by alphaherpesviruses: integrity of the tegument does not depend upon the presence of capsid or envelope. J. Gen. Virol. **73**:267–276.

32. **McLean, C., A. Buckmaster, D. Hancock, A. Buchan, A. Fuller, and A. Minson.** 1982. Monoclonal antibodies to three non-glycosylated antigens of herpes simplex virus type 2. J. Gen. Virol. **63**:297–305.

33. **McLean, G., F. Rixon, N. Langeland, L. Haarr, and H. Marsden.** 1990. Identification and characterization of the virion protein products of herpes simplex virus type 1 gene UL47. J. Gen. Virol. **71**:2953–2960.

34. **McNabb, D. S., and R. J. Courtney.** 1992. Characterization of the large

tegument protein (ICP1/2) of herpes simplex virus type 1. Virology **190**:221–232.

35. **Meredith, D. M., J. A. Lindsay, I. W. Halliburton, and G. R. Whittaker.** 1991. Post-translational modification of the tegument poteins (VP13 and 14) of herpes simplex virus type-1 by glycosylation and phosphorylation. J. Gen. Virol. **72**:2771–2775.

36. **Mettenleiter, T. C.** 2002. Herpesvirus assembly and egress. J. Virol. **76**:1537–1547.

37. **Miranda-Saksena, M., P. J. Armati, R. A. Boadle, D. J. Holland, and A. L. Cunningham.** 2000. Anterograde transport of herpes simplex virus type 1 in cultured, dissociated human and rat dorsal root ganglion neurons. J. Virol. **74**:1827–1839.

38. **Morrison, E. E., A. J. Stevenson, Y. F. Wang, and D. M. Meredith.** 1998. Differences in the intracellular localisation and fate of herpes simplex virus tegument proteins in the infection of Vero cells. J. Gen. Virol. **79**:2515–2528.

39. **Orci, L., M. Tagaya, M. Amherdt, J. Perrelet, J. G. Donaldson, J. Lippincott-Shwartz, R. D. Klausner, and J. E. Rothman.** 1991. Brefeldin A, a drug that blocks secretion, pevents the assembly of non-clathrin-coated buds on Golgi cisternae. Cell **64**:1183–1195.

40. **Penfold, M. E. T., P. A. Armati, and A. L. Cunningham.** 1994. Axonal transport of herpes simplex virions to epidermal cells: evidence for a specialized mode of virus tranport and assembly. Proc. Natl. Acad. Sci. USA **91**:6529–6533.

41. **Radsak, K., M. Eickmann, T. Mockenhaupt, E. Bogner, H. Kern, A. EisHübinger, and M. Reschke.** 1996. Retrieval of human cytomegalovirus glycoprotein B from the infected cell surface for virus envelopment. Arch. Virol. **141**:557–572.

42. **Rixon, F. J., C. Addison, and J. McLauchlan.** 1992. Assembly of enveloped tegument structures (L particles) can occur independently of virion maturation in herpes simplex virus type 1-infected cells. J. Gen. Virol. **73**:277–284.

43. **Robinson, M. S., and T. E. Kreis.** 1992. Recruitment of coat proteins onto Golgi membranes in intact and permeabilized cells: effects of brefeldin A and G protein activators. Cell **69**:129–133.

44. **Roffman, E., J. P. Albert, J. P. Goff, and N. Frenkel.** 1990. Putative site for the acquisition of human herpesvirus 6 virion tegument. J. Virol. **64**:6308–6313.

45. **Roizman, B., and A. E. Sears.** 1996. Herpes simplex viruses and their replication, p. 2231–2296. *In* B. N. Fields, D. M. Knipe, and P. M. Howley (ed.), Fields virology, 3rd ed. Raven Press, Philadelphia, Pa.

46. **Schweizer, A. J., A. M. Fransen, T. Bachi, L. Ginsel, and H.-P. Hauri.** 1988. Identification, by monoclonal antibody, of a 53-kDa protein associated with a tubulo-vesicular compartment at the *cis*-side of the Golgi apparatus. J. Cell Biol. **107**:1643–1653.

47. **Skepper, J. N., A. Whiteley, H. Browne, and A. Minson.** 2001. Herpes simplex virus nucleocapsids mature to progeny virion by an envelopment→ deenvelopment→reenvelopment pathway. J. Virol. **75**:5697–5702.

48. **Stackpole, C. W.** 1969. Herpes-type virus of the frog renal adenocarcinoma: virus development in tumor transplants maintained at low temperature. J. Virol. **4**:75–93.

49. **Tomishima, M. J., and L. W. Enquist.** 2001. A conserved alphaherpesvirus protein necessary for axonal localization of viral membrane proteins. J. Cell Biol. **154**:741–752.

50. **Whealy, J. P., M. E. Card, R. P. Meade, A. K. Robbins, and L. W. Enquist.** 1991. Effect of brefeldin A on alphaherpesvirus membrane protein glycosylation and virus egress. J. Virol. **65**:1066–1081.

51. **Whiteley, A., B. Bruun, T. Minson, and H. Browne.** 1999. Effects of targeting herpes simplex virus type 1 gD to the endoplasmic reticulum and *trans*-Golgi network. J. Virol. **73**:9515–9520.

52. **Whittaker, G. R., M. P. Riggio, I. W. Halliburton, R. A. Killington, G. P. Allen, and D. M. Meredith.** 1991. Antigenic and protein sequence homology between VP13/14 and a herpes simplex type 1 tegument protein, and gp10, a glycoprotein of equine herpesviruses 1 and 4. J. Virol. **65**:2320–2326.

53. **Yao, F., and R. J. Courtney.** 1989. A major transcriptional regulatory protein (ICP4) of herpes simplex virus type 1 is associated with purified virions. J. Virol. **63**:3338–3344.

54. **Yao, F., and R. J. Courtney.** 1992. Association of ICP0 with but not ICP27 with purified virions of herpes herpes simplex virus type 1 virions. J. Virol. **66**:2709–2716.

55. **Zhou, Z. H., D. Hua Chen, J. Jakana, F. Rixon, and W. Chiu.** 1999. Visualization of tegument-capsid interactions and DNA in intact herpes simplex virus type 1 virions. J. Virol. **73**:3210–3218.

56. **Zhu, Z., M. D. Gershon, Y. Hao, R. T. Ambron, C. A. Gabel, and A. A. Gershon.** 1995. Envelopment of varicella-zoster virus: targeting of viral glycoproteins to the *trans*-Golgi network. J. Virol. **69**:7951–7959.